

# Three-dimensional simulations of a vertically vibrated granular bed including interstitial air

V. Idler,<sup>1,2,\*</sup> I. Sánchez,<sup>1,†</sup> R. Paredes,<sup>1,‡</sup> G. Gutiérrez,<sup>2</sup> L. I. Reyes,<sup>2</sup> and R. Botet<sup>3</sup>

<sup>1</sup>*Centro de Física, Instituto Venezolano de Investigaciones Científicas, Apartado Postal 21827, Caracas 1020-A, Venezuela*

<sup>2</sup>*Departamento de Física, Universidad Simón Bolívar, Apartado 89000, Caracas 1080-A, Venezuela*

<sup>3</sup>*Laboratoire de Physique des Solides Bâtiment 510, CNRS UMR8502, Université Paris-Sud, F-91405 Orsay, France*

(Received 1 February 2009; published 6 May 2009)

We present a numerical study of the effect of interstitial air on a vertically vibrated granular bed within one period of oscillation. We use a three-dimensional molecular-dynamics simulation including air phenomenologically. The simulations are validated with experiments made with spherical glass beads in a rectangular container. After validation, results are reported for a granular column of 9000 grains and  $\approx 50$  layers deep (at rest), agitated with a sinusoidal excitation with maximal acceleration  $4.7g$  at  $11.7$  Hz. We report the evolution of density, granular temperature, and coordination number within a vibration cycle, and the effect of interstitial air on those parameters. In three-dimensional computer simulations we found that the presence of interstitial air can promote the collective motion of the granular material as a whole.

DOI: [10.1103/PhysRevE.79.051301](https://doi.org/10.1103/PhysRevE.79.051301)

PACS number(s): 45.70.-n, 47.57.Gc

## I. INTRODUCTION

Granular materials are used in numerous industrial processes, and further research is needed to improve the efficiency and reach of actual technological capabilities [1]. The physics of granular systems has been avidly studied in the last decades because of the several interesting phenomena that take place when they are excited in some way (by vibration, rotation, shearing, fluid injection, etc.), and because of the challenge presented by adequately modeling and effectively predicting their behavior. This recent boom of basic research has begun to pay some results [2]. Granular materials together with other materials such as foams and pastes have been called “soft matter.” There are good reviews about their physical interest, and we refer the reader to them [3–6].

Vertical vibration is one of the most used methods for injecting energy in a granular system, both in real manufacturing processes and in research studies. Depending on the intensity of the vibration and on the characteristic of the granular medium, there are many interesting phenomena such as pattern formation [7–9], convection [10,11], segregation [12–15], bunkering or heaping [16–18], and surface waves [19]. Besides interest in a particular effect, there are reported studies aiming at identifying the different regimes that can be achieved by shaking [20–22], and at adequately modeling a vertically vibrated bed [23–26] (there is extensive work on dilute systems and implications of kinetic theory, which we will not address here). Their references will lead the interested reader to older research published in German, Russian, and Japanese.

The role of interstitial fluid (typically air) in vibrated bed phenomena has been noted as determinant in the dynamic response of the granular bed to agitation. For example, Pak *et al.* [27] showed how convection and heaping are greatly reduced in vacuum; Faraday tilting has been related to the

flow of air through the bed [28] and has been studied also with water as the interstitial fluid [29]. Segregation is well affected by the presence of air [30–32] and density related effects as reverse buoyancy disappear in vacuum [33]. The fluid-grain interaction, well understood, could be used to adequately rescale a particular configuration in order to avoid or to enhance some effect (convection, segregation, vertical transport) [34,35]. Thus, there is a need for inclusion of the grain-fluid interaction in numerical simulations of vibrated granular beds if we want to reproduce effects such as reverse buoyancy, which are related to a strong air-bed interaction. This paper addresses the problem of studying the change in the internal structure of the bed when air affects its macroscopic behavior.

Distinct element simulation (DEM) has become the standard computational tool for modeling granular materials. The interested reader is referred to the recent reviews of Zhu and co-workers [36,37] for a wider point of view of the technique and its applications. When it comes to vertically vibrated granular materials, there is plenty of work dedicated to spherical grains in vacuum [38–40] but, generally in the physics literature, computer simulations of granular materials rarely take into account the interstitial fluid. The inclusion of an interstitial fluid was first used to model fluidized beds, where the fluid-grain interaction is determinant [41,42]. More recently, Biswas *et al.* [43] modeled segregation under vertical vibration in a system with air as the interstitial fluid and found qualitative similar results as the ones reported in previous experimental work [44]. Our paper aims at studying the effect of interstitial air on the dynamical structure of a vertically vibrated bed using a similar model as that of [43], carefully tuned to match our own experimental observations.

This paper is organized as follows: in Sec. II we describe our simulation model. Section III explains how we calibrated our simulations with experimental observations. In Sec. IV we will focus on the temporal evolution of relevant properties within one cycle of oscillation of the system. Finally, Sec. V presents our closing remarks and conclusions.

\*vladimiridler-granular@yahoo.com

†ijsanche@ivic.ve

‡rparedes@ivic.ve

## II. COMPUTATIONAL MODEL

We use a three-dimensional (3D) molecular-dynamics (MD) simulation of soft spheres. The interaction contact force we choose is given by [45] (this force is derived from Cundall and Strack's force model [46]):

$$\mathbf{F}_{ij} = \{k_n(R_i + R_j - r_{ij}) - \gamma_n m(\mathbf{v}_{ij} \cdot \hat{\mathbf{n}})\} \hat{\mathbf{n}} - \text{sgn}(v_{\text{rel}}) \{ \min(\gamma_s m |v_{\text{rel}}|, \mu_f |\mathbf{F} \cdot \hat{\mathbf{n}}|) \} \hat{\mathbf{s}}, \quad (1)$$

where  $R_i$  is radius of the  $i$ th particle,  $\vec{r}_{ij} = r_{ij} \hat{\mathbf{n}}$  is the vector connecting the centers of the  $i$ th and  $j$ th particles,  $v_{\text{rel}} = \mathbf{v}_{ij} \cdot \hat{\mathbf{s}}$ , and  $\hat{\mathbf{s}}$  is a unitary vector perpendicular to  $\hat{\mathbf{n}}$  [47]. The first term accounts for the elastic interactions during contact. The second is due to viscous forces associated to normal deformations proportional to the collision velocity. The last term represents the shear friction among particles.  $m = m_i m_j / (m_i + m_j)$  is the reduced mass. The coefficients  $\gamma_n$  and  $\gamma_s$  assure inelasticity in the collisions, and are taken to be equal (for simplicity) [48].  $\mu_f$  is the standard static friction coefficient, we take it as 0.5.  $k_n$  is the elastic constant of the particles and is chosen to make sure the superposition between particles is appreciably smaller than the radii. The typical time scale is the collision time given by

$$t_{\text{col}} = \frac{2\pi}{(k_n/m - \gamma_n^2/4)^{1/2}}. \quad (2)$$

As our iteration time we used  $\Delta t \approx t_{\text{col}}/500$  [49]. This particular value allowed us to grant stability in the resolution of differential equations [50]. We used a uniform distribution of diameters, with a maximum deviation of 10%.

We include air phenomenologically using the approach of Biswas *et al.* [43]. They simplify the model of McNamara *et al.* [42] assuming air as an incompressible fluid. With the above in mind, we take the force due to interstitial air on each particle as

$$\vec{F}_i^a = - \frac{\mu}{\kappa(\rho_s)\rho_n} (\vec{v}_a - \vec{v}_i), \quad (3)$$

where  $v_i$  is the vertical velocity of the  $i$ th particle,  $v_a$  is the velocity of the gas outside the granular bed, interstitial gas velocity,  $\rho_n$  is the numeric density,  $\rho_s$  is the packing fraction,  $\kappa$  is the local permeability, and  $\mu$  is the air viscosity. To compute the permeability, we used the Karman-Kozeny relation  $\kappa = \frac{d^2}{K} \frac{(1-\rho_s)^3}{\rho_s^2}$ , where  $K$  is an empirical constant and  $d$  is the mean grain diameter. The numeric density is related to the packing fraction by  $\rho_n = \rho_s / V_g$  (with  $V_g$  as the average grain volume). Reorganizing we obtain

$$\vec{F}_i^a = - \alpha(\mu, d, \phi) (\vec{v}_i - \vec{v}_a), \quad (4)$$

with the coefficient  $\alpha$  given by

$$\alpha = \frac{Kd\mu\pi(1-\phi)}{6\phi^3}, \quad (5)$$

and  $\phi = 1 - \rho_s$  is the porosity. To obtain  $\vec{F}_i^a$  we start by considering the granular column as a static porous medium at each time step. Here we set apart from the approach of Biswas *et al.* [43] in that we use a local  $\alpha$  (computed by con-

sidering the packing fraction in a neighborhood around each grain) while they considered a global one. This difference in how the porosity is taken has proven to be useful in simulating other phenomena in vertically vibrated granular beds [51]. We choose an upper bound for the value of the local porosity because the Karman-Kozeny relation is known to fail at high porosity [42]. As such we take  $\phi = 0.75$  as an upper threshold and replace all cases with  $\phi > 0.75$  by 0.75. Finally,  $v_a$  equals the velocity of the container because air is taken as an incompressible fluid.

Grains were placed in a rectangular container with dimensions  $L_x$ ,  $L_y$ , and  $L_z$  (each of them proportional to the mean particle diameter), periodic boundary conditions in the axes  $x$  and  $z$ , and hard walls on  $y=0$  and  $y=L_y$  (we take  $y$  as the vertical axis).  $L_y$  is taken large enough to avoid grains reaching the ceiling of the container during agitation. Simulations are started from an initial configuration in which all the grains are resting at the container bottom. This condition is achieved by randomly placing the grains in the container, with random velocities, without vibrating the container, and letting the system evolve under gravity.

## III. CALIBRATION

In order to calibrate the simulations we decided to measure the size of the gap between the bottom of the granular column and the bottom of the container as a function of the phase of oscillation, and compare it with experimental results. The gap represents a comfortable experimental macroscopic observable and that is the main reason why we chose it as the calibration parameter. Experiments were performed with a simple oscillator made out of two mechanically coupled loudspeakers, driven by an amplified function generator. The experimental container was made of acrylic with the same dimensions considered in the simulations. To measure the gap, high-speed photography together with video analyzing techniques were used. Glass spheres of five different average diameters were used (1–5 mm), with size dispersion of the order of 10%. Antistatic spray was applied to the spheres prior to each set of experiments. Also rice, mustard, and parapara [52] seeds were used in experiments. Results correspond to a typical experimental run in which more than 100 cycles are averaged.

We adjusted the effect of air in the simulations by changing the constant  $K$  in Eq. (5) in order to emulate the experimental findings. We increased its value if the simulations were overestimating the gap and reduce it if the simulations were underestimating the gap. Figure 1 shows a good agreement between experiments and simulations for 12 Hz, two different values of  $\Gamma = A\omega^2/g$ , and three different grain diameters (2–4 mm). Both the quantitative values and the functional shape are very similar. There is a little difference at landing, as expected from the incompressibility assumption. This agreement was found with a constant  $K=495$ . This value gave us a window in the parameter domain ( $\Gamma$ , frequency, amplitude, and  $d$ ) in which our model quantitatively reproduces the experimental observations. If we move out of this window, one has to readjust the value of  $K$  in order to match the experimental results. This limits our range of ex-

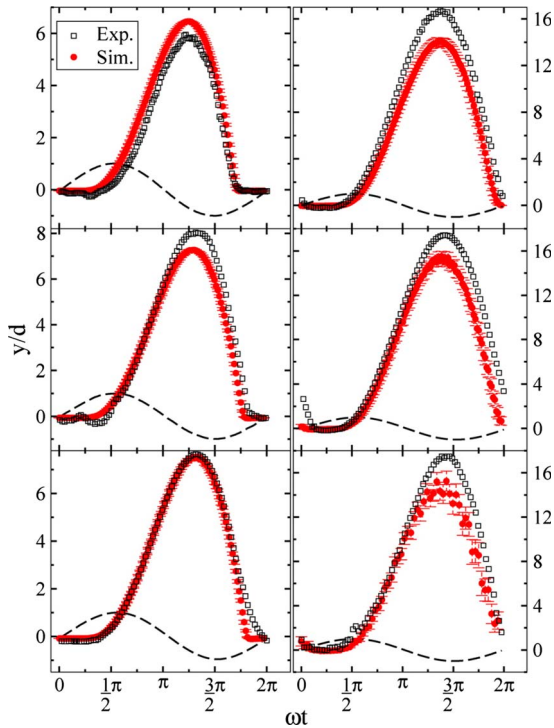


FIG. 1. (Color online) Gap height as a function of phase for grains of density  $\rho_g=2200 \text{ kg/m}^3$  at a vibration frequency of 12 Hz. Both experiments with spherical glass beads (squares) and MD simulations (bold circles) are shown.  $\Gamma=2.84$  (left column) and  $\Gamma=4.83$  (right column).  $d=2$  (first row), 3 (second row), and 4 mm (third row). Using  $K=495$ , we obtained a “window” in the parameter space where the simulations adequately reproduce the experimental gap.

trapolation but we gain confidence in the interval studied. Of course, this domain of parameters could be extended if we are interested only in qualitative results.

To have an idea of the accuracy of the model, Fig. 2 shows measures of the experimental maximum gap  $\Delta_{\max}$  compared with simulations for different  $\Gamma$ , frequency, and grain diameter, keeping  $\rho_g$  constant and the coefficient  $K=495$ . As can be seen, the worst case scenarios for this value of  $K$  is when  $d=1 \text{ mm}$  and when  $\Gamma$  is large. Even in those cases, it is possible to obtain a good match with experiments

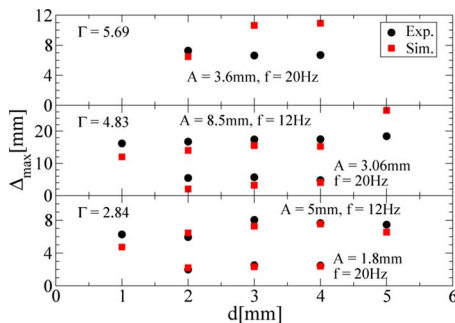


FIG. 2. (Color online) Maximum gap height as a function of grain diameter  $d$  for different parameters. Using  $K=495$  as the Karman-Kozeny constant, we obtain a good match between experiments and simulations for most of the points explored.

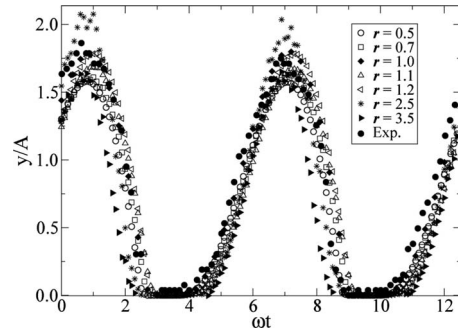


FIG. 3. Adimensional gap for different simulations with 2000 particles of  $d=2 \text{ mm}$  and  $\rho_g=2200 \text{ kg/m}^3$ , and varying  $A$ ,  $f=r \times 11.7 \text{ Hz}$ , and  $K$  so as to keep  $\Gamma$  and  $\tau_k$  constant. Experimental results for mustard seeds at  $f=11.7 \text{ Hz}$  and the same  $\Gamma$  are also shown. Gutiérrez *et al.* [54] predicted a collapse of the curves while our simulations show a fair degree of collapse.

if another value of  $K$  is chosen. In the following section, we will discuss simulations with  $K=495$  and  $\Gamma=4.7$ , i.e., inside the region of good match between experiments and simulations.

An interesting feature is that one of the assumptions made by our computational model is the same as that made by the much simpler one-dimensional vibrated piston model proposed by Kroll [53], i.e., air is taken as an incompressible fluid. Kroll’s model makes a further assumption: the granular medium is taken as a porous solid block, and its porosity and permeability are constant. Our simulations allow for variations in the package porosity and permeability both in space and time. If we compare the predictions of Kroll’s model with the results of our simulations we can see that the latter are closer to the experimental results. This shows that, although taking air as an incompressible fluid is a strong assumption, the local and instantaneous evaluation of the porosity results in a significant improvement [51]. In spite of it being unable to adequately reproduce the experimental results, Kroll’s model offers a useful qualitative prediction: that the adimensional gap (defined as the gap height over the amplitude) is only a function of two adimensional parameters: one related to the intensity of energy injection ( $\Gamma$ ) and another related to the dissipative characteristics of the system ( $\tau_k=\omega\kappa\rho/\mu$ , see [34] for an explicit derivation). If we rescale the gap obtained in the simulations and vary several of the parameters, we can see that there is not a perfect collapse but rather a fair one (see Fig. 3). This deviation from the predictions of Kroll’s model can be viewed as an improvement in the effort to emulate the actual granular behavior.

It is also important to point out the fact that experimentally we have found the shape of the grains to be a noncrucial parameter. Both rice and mustard seeds show a very similar gap for a given set of vibration parameters. The bulk density of rice and mustard seeds is  $\approx 1400 \text{ kg/m}^3$  but their shape is clearly dissimilar, mustard seeds being quasispherical and rice grains being elongated. Also sand and glass microspheres faceted through the same pair of sieves show a very similar gap. Thus, our simulation of spherical particles, although idealized, can be used to model irregularly shaped grains, at least to some degree.

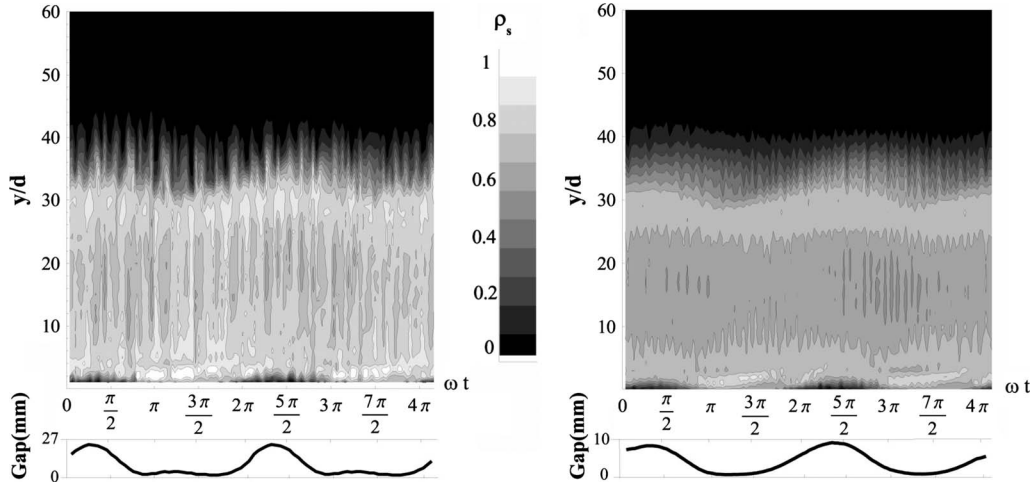


FIG. 4. Packing fraction as a function of height and phase for a simulation of 4500 particles with  $d=10$  mm, grain density  $\rho_g = 2200$  kg/m<sup>3</sup>, amplitude  $A=8.5$  mm, and frequency  $f=11.7$  Hz. *Left*: with air. *Right*: without air. Both cases show collective condensed motion with a bulk for layers 30 and below.

**IV. RESULTS**

We will now discuss the behavior of several local properties of the system as a function of the distance  $y$  from the bottom of the container and time. In particular we studied the density, the granular temperature, and the coordination number. We will report average values over horizontal layers of one-particle diameter in height. We will pay special attention to the effect of air in those parameters. As we commented in the previous section, simulations with air means taking  $K = 495$  in Eq. (5). Without air means taking the coefficient  $\alpha = 0$  in Eq. (4).

**A. Density profiles**

Depending on the properties of the granular medium being studied and the vibration parameters used, it is possible to achieve a regime in which the granular package behaves as a whole, bouncing periodically on the bottom of the container, or (if, for example, the intensity of vibration is large enough, and/or the dissipation properties of the grains are small enough) it is possible to obtain a granular gas filling the container (see, for example, [55,56]). Previous computational and experimental studies identified the number of grains (or the number of layers) and the coefficient of restitution of the grains as the parameters determining the change from one regime to another [57]. Naturally, other parameters such as grain density, humidity, and inelastic collisions may also influence the collective behavior of the granular material. The net effect of air is to promote the condensed motion of the granular package as a whole, acting as a dissipative factor.

First let us take a look at a case in which air effects are not very important. Figure 4 shows the density as a function of time and height for 4500 grains with diameter  $d = 10$  mm and density  $\rho_g = 2200$  kg/m<sup>3</sup>. In principle both cases with and without air seem alike but it is possible to point out some differences. The gap is larger in the case with air, something that could be counterintuitive. This is due to a

small degree of gasification in the case without air. In both cases, a stable bulk appears with packing fraction greater than the random loose packing for monodisperse spheres ( $\approx 0.61$  [58–60]). The bulk is denser in the case with air. Even though these grains are large and quite dense, the effects of interstitial air can already be seen, resulting in a promotion of the collective condensed motion of the column. In fact, the case with air better resembles the motion of an inelastic point mass than the case without air. However, in this particular case, the combination of number of layers and grain density is the fundamental reason of the formation of a bulk.

To see the vertical variation in density in a clearer way, we plot in Fig. 5 density profiles at four different phases. In all cases a plateau is seen corresponding to the bulk with packing fraction around 0.6 although the edges of the bulk reach numeric densities of 0.7 (higher than the random close packing for spheres which is reported as  $0.6366 \pm 0.0005$  in [60]). Remember that we are using a homogeneous distribution of diameters, which allow us to get higher filling fractions than with monodisperse grains. The case when the column is in contact with the container’s bottom (solid

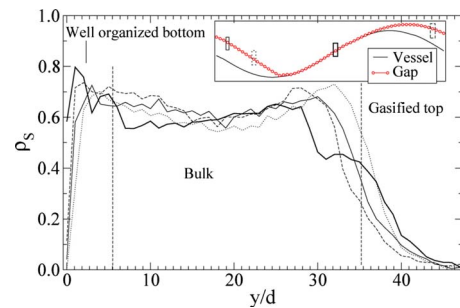


FIG. 5. (Color online) Vertical density profiles at four different phase values for the data of Fig. 4 left. The inset shows the phase position of each curve. A bouncing bulk is observed with fairly stable density in time and height but with fluctuations of the order of 0.1.

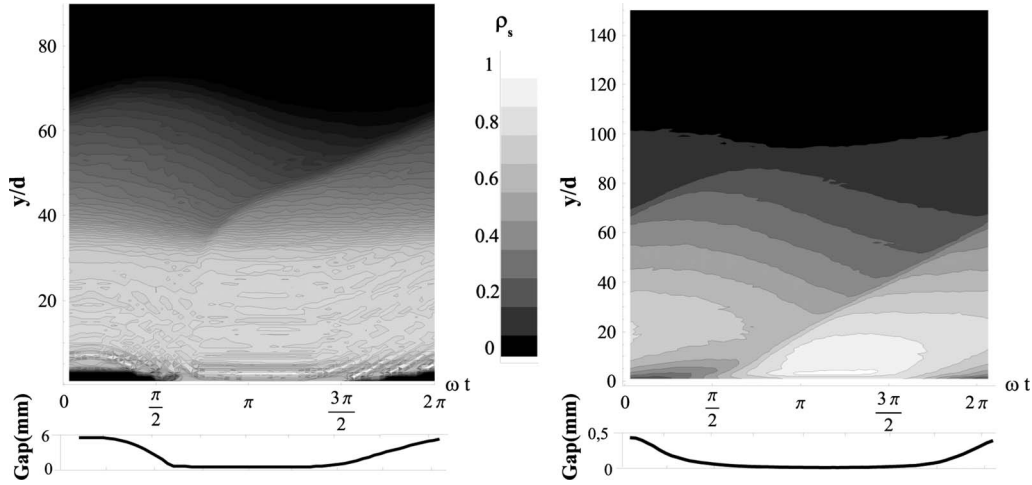


FIG. 6. Packing fraction as a function of height and phase for a simulation of 9000 particles with  $d=2$  mm, grain density  $\rho_g = 220$  kg/m<sup>3</sup>, amplitude  $A=8.5$  mm, and frequency  $f=11.7$  Hz. *Left*: with air. *Right*: without air. Here, a bulk appears only in the case with air for layers 30 and below. The case without air is highly gasified.

continuous line) shows a peak in packing fraction, reaching values greater than the hexagonal close packing for monodisperse spheres ( $\approx 0.74$ ). On top of the bulk (layers 35 and up) there is a ten layer deep gasified zone in which the packing fraction drops to zero. In experiments, if one inserts a rod into the top of the container while vibrating, it is possible to discriminate the gaseous top of the column from the denser bulk by the resistance to penetration.

Now, let us take a look at a case where air effects are enhanced. Simulations of very small grains are difficult because the number of grains grow, the characteristic time decreases, and then simulation time increases. For this reason, we decided to simulate grains of  $d=2$  mm and a very low density of  $\rho_g=220$  kg/m<sup>3</sup> (ten times lower than regular soda-lime glass beads of the same size). In this way we could enhance the dissipative effect of the interstitial fluid and explore its consequences.

Figure 6 shows the density as a function of time and height for 9000 grains with diameter  $d=2$  mm and density  $\rho_g=220$  kg/m<sup>3</sup>. Here, both cases with and without air are clearly different. The case without air is gasified; thus there is almost no gap at the bottom, there is no bulk, and there is a significant bed expansion (there are grains reaching heights of 100 layers). This higher degree of gasification achieved (if one compares it to the case of Fig. 4) is due to the low grain density used, even though we doubled the number of grains and maintain the same coefficient of restitution. The case with air (left side of Fig. 6) shows a bulk bouncing periodically on the bottom of the container. As can be appreciated in Fig. 7, this time the bulk is shorter in height than in the case of Fig. 4, spanning about 20 layers. The mean packing fraction of this bulk  $\approx 0.74$  is greater than the case of Fig. 4 because the compacting effect of air is intensified due to the low grain density used in this case [61]. In fact, the density of the bulk is almost constant comparing it with the case of Fig. 5. Observing the evolution of the density, we have a homogeneous and stable bouncing bulk when the effect of the air is taken into account in the simulations. On top of the bulk, there is a larger gasified dilute zone of low density,

starting around layer 35 and spanning about 30 layers. The density of this gas reduces monotonically with  $y$ .

Both cases in Fig. 6 (with and without air) show the appearance of a density wave, a compaction front that starts at the bottom of the column when it lands on the container bottom and travels upward through the granular package, and whose propagation characteristics are affected dramatically by the presence of air. In the absence of air, the compaction front travels almost at constant speed of roughly 2 m/s through the granular medium. This wave propagation has been observed by other DEM simulations without air [40,62,63] and experiments in which air effects are negligible [55,64]. Under air effects, as in the left side of Fig. 6, the density wave velocity is not constant in height. It travels extremely fast through a solid bulk (from layer 1 to 30) and then slows down when it reaches the granular gas on the top of the column, where it travels at a speed of  $\approx 1.4$  m/s.

Potapov and Campbell [65] performed simulations of a deep bed without including air and found no density waves. They argued that their choice of a linear contact model (linear-spring-dash pot) was the reason for their lack of density waves, as compared with Aoki and Akiyama's [62] study (whose simulation used a truncated Lennard-Jones contact).

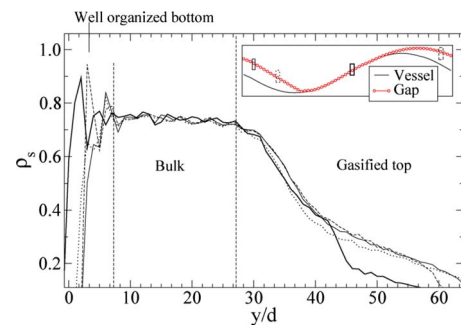


FIG. 7. (Color online) Vertical density profiles at four different phase values for the data of Fig. 6 left. The inset shows the phase position of each curve. The bulk is denser and more stable than the one in Fig. 5.

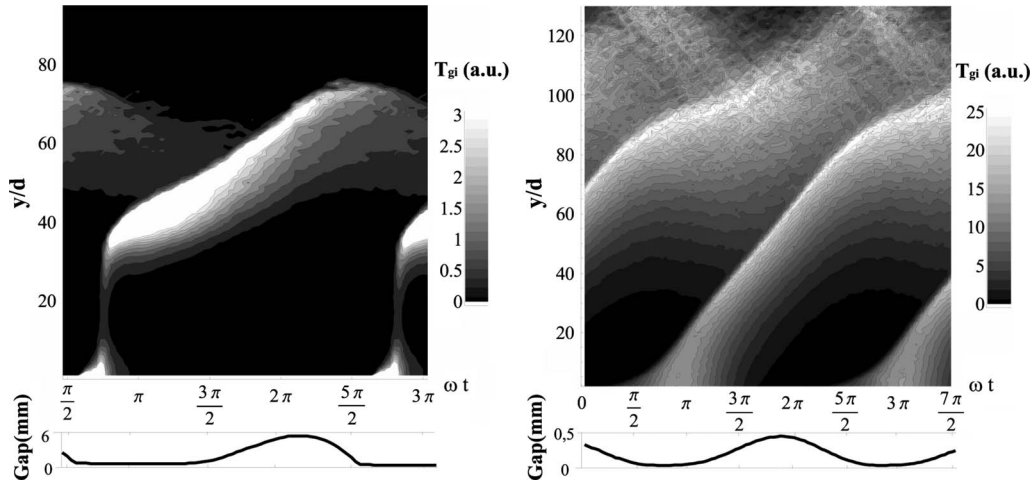


FIG. 8. Temperature as a function of height and phase for a simulation of 9000 particles with  $d=2$  mm, grain density  $\rho_g=220$  kg/m<sup>3</sup>, amplitude  $A=8.5$  mm, and frequency  $f=11.7$  Hz. *Left*: with air. The bulk is appreciably colder than the gas above. The granular temperature shows a peak corresponding with the phase in which the granular package lands on the container floor. This shows a rapid transfer of energy through the bulk to the gas, where it is slowly dispersed. *Right*: without air. The system is gasified with an overall temperature much larger than the case with air. The kinetic energy is slowly transferred from the bottom to the top, where it scatters.

As we observe the density waves using a linear contact model, we can state that the reason has to be somewhere else. It is more probable that the absence of density waves in [65] is due to their small amplitude of  $\approx 0.3$  diameters, resulting in a granular package that resembles a fluid but does not rebound on the plate as a solid column. Our simulations and those of Aoki and Akiyama [62] have values of  $\Gamma$  similar to those of Potapov and Campbell [65] but use amplitudes greater than one grain diameter.

**B. Temperature profiles**

The extensive study on granular gases has positioned the granular temperature as an important parameter. Typically the granular temperature is taken as a measure of the kinetic energy of the system. We define the adimensional granular temperature for a layer  $i$  as

$$T_{gi} = \langle v^2 \rangle_i = \langle v_x^2 + v_z^2 + (v_y - \langle v_y \rangle_i)^2 \rangle_i, \quad (6)$$

where  $y$  indicates the vertical direction, and  $x$  and  $z$  the orthogonal ones, and  $\langle \rangle_i$  indicates average on all the particles in the layer  $i$ . We found that the granular temperature associated with a particular direction has the same qualitative behavior, varying only in magnitude (as in [66,67]). Thus for simplicity we will discuss only the vertical component of the temperature:

$$T_{gyi} = \langle (v_y - \langle v_y \rangle_i)^2 \rangle_i. \quad (7)$$

The source of kinetic energy in vibrated systems is basically the motion of the container. Monitoring the granular temperature gives us a clue about the energy transfer between the plate and the granular medium. Figure 8 shows the temperature as a function of time and height for 9000 grains with diameter  $d=2$  mm and density  $\rho_g=220$  kg/m<sup>3</sup> (the same system as in Fig. 6). In general one can appreciate that there are temperature rises related to the advance of the com-

paction wave and the agitated upper part of the column. The case without air shows cold zones at the bottom of the column temporarily disrupted by the passing of the compaction wave. There is a hotter zone at the upper part of the column (layers 60 and up). Here we can see how the compaction wave slows down when it approaches layer 90, indicating a clear change in the properties of the medium. It is important to point out that the hot zone in layers over 100 is very dilute, only a few particles contribute to the average in each layer (as can be seen in the right side of Fig. 6). The case with air shows temperatures that are one order of magnitude lower than in the case without air. The bulk remains cold during most of the cycle, except just at the moment of landing. At this phase there is a local increase in temperature at the bottom that travels almost instantaneously to the upper part of the bulk, where it slows down noticeably and dissipates in the gaseous top. If ones looks deeper into the bulk, as can be seen in Fig. 9, it is possible to appreciate a structure (although fluctuations occur at a very small scale). Inside the bulk, the core is colder than the top and bottom edges, and the colder phases correspond to the ones after the maximum gap is reached. Nevertheless, when compared to the whole system, the temperature of the bulk is practically homogeneous.

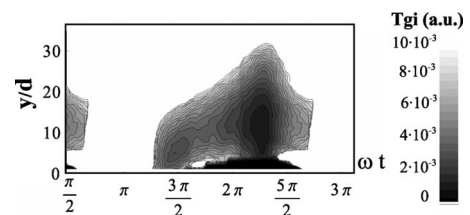


FIG. 9. Detailed variation in temperature inside the bulk of the left side of Fig. 8. Observing the gray scale, this figure shows a clear evidence of the homogeneity of the bulk temperature in the case with air.

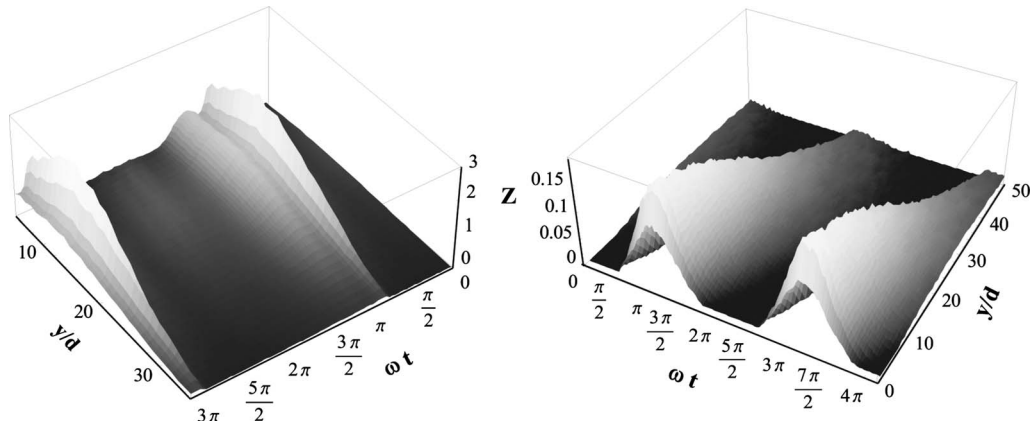


FIG. 10. Coordination number  $Z$  as a function of height and phase for a simulation of 9000 particles with  $d=2$  mm, grain density  $\rho_g = 220$  kg/m<sup>3</sup>, amplitude  $A=8.5$  mm, and frequency  $f=11.7$  Hz. *Left*: with air.  $Z$  remains close to zero while the package is in flight. It shows a peak corresponding to the peak in granular temperature. *Right*: without air.  $Z$  remains close to zero during the whole period of oscillation (as expected in a gasified state).

As the granular temperature is directly related to grain mobility, we can conclude that the effect of air is compromising the mobility of individual grains. It promotes collective behavior, the definition of a bulk inside which the relative motion of grains is negligible. The main source of mobility in the column is the compaction front associated with the impact with the bottom of the container (as was also found by [62,68]). In our set of vibration parameters used, kinetic energy is transferred smoothly through the column in the case without air, and abruptly in the case with air.

### C. Coordination number

The coordination number  $Z$  (defined as the number of contacts per particle) provides information about the local structure of the granular material. Previous simulations have shown that the average  $Z$  for a stable static column of monodisperse spheres is  $\approx 4.5$  for a packing fraction of  $\approx 0.61$  [69,70]. In the initial state of our simulations, we obtain  $Z \approx 6$  with the column at rest (our system is not monodisperse).

Let us discuss the behavior of  $Z$  when air effects are drastic ( $d=2$  mm,  $\rho_g=220$  kg/m<sup>3</sup>). Figure 10 right shows how, for the case without air,  $Z$  remains lower than one during the whole period of oscillation. This indicates that most of the particles move alone, without contacting its neighbors (a sign of gasification). However, in this plot, we can observe a region in which  $Z$  is maximum. This maximum decreases with height as the phase increases. This behavior agrees with the compaction wave traveling through the medium, which is also observed in Fig. 8 right.

Figure 10 left shows the behavior of  $Z$  in the presence of air. We can see a flat region of low  $Z$  coinciding with the phase when the gap is different than zero [the gap is plotted in Fig. 8]. In the region where the gap is zero ( $\pi/2 < \omega t < 3\pi/2$ ), the value of  $Z$  is much greater. Specifically at the moment in which the column lands on the bottom plate, there is an abrupt increase in the coordination number. This peak, although it reaches  $\approx 3$ , does not reach the critical value of four necessary for there to be static mechanical equilibrium

[71]. If we remember the temperature plots of Fig. 8 left, there is a temperature increase traveling extremely fast to the upper part of the column. We can see how the peak in  $Z$  occurs almost simultaneously for the whole bulk. It is interesting to see that the package is able to transmit the collision energy to the gaseous top while presenting a small coordination number. This suggests the existence of a transmitting structure from the bottom to the top of the column. Another noticeable point is the second smaller peak that occurs right after the first peak (the one which coincides with the column landing). This is something that is not appreciated in the temperature or the packing fraction. This second peak was also observed by [72].

Comparing the results from [72] with the plot in Fig. 10 left is not direct. The parameters used by [72] promote the collective motion of the package (assuming  $d=2$  mm, their frequency is  $\approx 7.5$  Hz, and their amplitude is  $\approx 15$  mm). Instead, our simulation without air is more gasified. The effect of air in our system changes the gasified state to a collective one, comparable to the results of [72]. As an additional comment, Sun *et al.* [72] studied the effect of wall friction on the behavior of  $Z$  in a vertically agitated system. They found that frictionless walls produced a noncyclic  $Z$  while walls with a friction coefficient of 0.5 produced a cyclically varying  $Z$ , with peaks associated to phases in which the granular package is static. Our system has periodic boundary conditions, and still achieves a cyclic  $Z$ .

We have to note that the effect of air is not so trivial as to increase the average  $Z$ . If we have a configuration without air in which there is collective motion, as in Fig. 11 bottom, we obtain values of  $Z$  that reach five. Including air lowers the overall value of  $Z$ , as can be seen in Fig. 11 top. In this case, air is not acting as a compacting figure. This effect shown by our raw model could be related in real systems to the air flow around the particles tending to reduce the contact among them. In fact, Fig. 10 left shows that the maximum  $Z$  is not reached at the bottom of the package. This is due to the cushioning effect of the upward airflow.

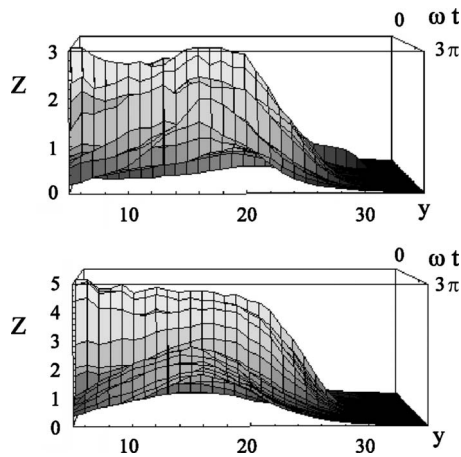


FIG. 11. Coordination number as a function of height and phase for a simulation of 4500 particles with  $d=10$  mm, grain density  $\rho_g=220$  kg/m<sup>3</sup>, amplitude  $A=8.5$  mm, and frequency  $f=11.7$  Hz. *Top*: with air. *Bottom*: without air. This particular configuration shows collective condensed motion in the absence of air. The effect of air, in this case, is to reduce the overall value of  $Z$ .

## V. SUMMARY

We have presented 3D molecular-dynamics simulations of a vertically vibrated column of grains, taking into account the effect of interstitial air. The simulations were successfully validated with experimental observations of the gap formed between the container floor and the bottom of the granular column. After validating this global parameter (the gap), we were able to use the simulations to locally explore physical parameters such as packing fraction, granular temperature, and coordination number.

Our main results apply to a system in which air effects determine the dynamics of the granular medium. We chose a system that in the absence of air was completely gasified.

When the effect of air was turned on in the simulations, it promoted the condensed motion of the granular column, enhancing the appearance of a dense bulk, crowned by a dilute gas. This bulk has a stable packing fraction of  $\approx 0.74$  both in phase and height. The bulk remains cold during most of the cycle with granular temperature near zero except just at the moment when the column collides with the container bottom. In that precise moment a compaction front propagates almost instantaneously through the bulk, originating a huge peak in the granular temperature. The promotion of collective motion of the grains due to air is reported in a three-dimensional computer simulation of a vibrated granular column.

Also, we have seen in such system that the coordination number remains close to zero when the package is in flight, and rises when it is in contact with the container floor. It shows a peak at the same phase as the granular temperature peak. This energy propagation is much slower when the system is gasified, as can be seen above the bulk, or in the case without air. This results, although being obtained for grains with low density and diameter of the order of millimeters, could be qualitatively similar to systems with larger densities and fine particles [34,35].

Before the end we have to point out that air does not always promote collective motion. Here, we showed some evidence of this for the case of a system which already shows collective condensed motion in the absence of air. When we include the effect of air, the coordination number decreases appreciably. In this case one of the effects of air is to reduce the contacts between grains. This is something that could be explored in future experiments.

## ACKNOWLEDGMENTS

This work has been done under the PCP-FONACIT Franco-Venezuelan Program: Dynamics and Statics of Granular Materials. This research was supported in part by Grant No. S1-200000624 and by DID of the Universidad Simón Bolívar.

- 
- [1] B. Ennis, J. Green, and R. Davies, *Chem. Eng. Prog.* **90**, 32 (1994).
  - [2] J. M. Ottino and D. V. Khakhar, *Powder Technol.* **121**, 117 (2001).
  - [3] P. G. de Gennes, *Rev. Mod. Phys.* **71**, S374 (1999).
  - [4] E. Clément, *Curr. Opin. Colloid Interface Sci.* **4**, 294 (1999).
  - [5] L. P. Kadanoff, *Rev. Mod. Phys.* **71**, 435 (1999).
  - [6] H. M. Jaeger, S. R. Nagel, and R. P. Behringer, *Rev. Mod. Phys.* **68**, 1259 (1996).
  - [7] S. Douady, S. Fauve, and C. Laroche, *Europhys. Lett.* **8**, 621 (1989).
  - [8] E. Clément, L. Vanel, J. Rajchenbach, and J. Duran, *Phys. Rev. E* **53**, 2972 (1996).
  - [9] F. Melo, P. B. Umbanhowar, and H. L. Swinney, *Phys. Rev. Lett.* **75**, 3838 (1995).
  - [10] Y-h. Taguchi, *Phys. Rev. Lett.* **69**, 1367 (1992).
  - [11] S. Hsiau and C. Chen, *Powder Technol.* **111**, 210 (2000).
  - [12] J. Williams, *Powder Technol.* **15**, 245 (1976).
  - [13] J. Ottino and D. Khakhar, *Annu. Rev. Fluid Mech.* **32**, 55 (2000).
  - [14] A. Rosato, D. Blackmore, N. Zhang, and Y. Lan, *Chem. Eng. Sci.* **57**, 265 (2002).
  - [15] A. Kudrolli, *Rep. Prog. Phys.* **67**, 209 (2004).
  - [16] P. Y. Lai, L. C. Jia, and C. K. Chan, *Phys. Rev. E* **61**, 5593 (2000).
  - [17] E. Clément, J. Duran, and J. Rajchenbach, *Phys. Rev. Lett.* **69**, 1189 (1992).
  - [18] T. Akiyama, K. Aoki, K. Yamamoto, and T. Yoshikawa, *Granular Matter* **1**, 15 (1998).
  - [19] H. K. Pak and R. P. Behringer, *Phys. Rev. Lett.* **71**, 1832 (1993).
  - [20] B. Thomas, M. Mason, Y. Liu, and A. Squires, *Powder Technol.* **57**, 267 (1989).
  - [21] B. Thomas, M. Mason, and A. Squires, *Powder Technol.* **111**, 34 (2000).
  - [22] S. Hsiau and S. Pan, *Powder Technol.* **96**, 219 (1998).

- [23] T. Akiyama and T. Naito, *Chem. Eng. Sci.* **42**, 1305 (1987).
- [24] T. Akiyama and H. Kurimoto, *Chem. Eng. Sci.* **43**, 2645 (1988).
- [25] W. Gray and G. Rhodes, *Powder Technol.* **6**, 271 (1972).
- [26] T. Akiyama and H. Kurimoto, *Chem. Eng. Sci.* **44**, 427 (1989).
- [27] H. K. Pak, E. Van Doorn, and R. P. Behringer, *Phys. Rev. Lett.* **74**, 4643 (1995).
- [28] B. Thomas and A. M. Squires, *Phys. Rev. Lett.* **81**, 574 (1998).
- [29] M. C. Leaper, A. J. Smith, Michael R. Swift, P. J. King, H. E. Webster, N. J. Miles, and S. W. Kingman, *Granular Matter* **7**, 57 (2005).
- [30] M. A. Naylor, M. R. Swift, and P. J. King, *Phys. Rev. E* **68**, 012301 (2003).
- [31] M. E. Mobius, X. Cheng, P. Eshuis, G. S. Karczmar, S. R. Nagel, and H. M. Jaeger, *Phys. Rev. E* **72**, 011304 (2005).
- [32] G. Gutiérrez, O. Pozo, L. Reyes, R. Paredes, J. Drake, and E. Ott, *Europhys. Lett.* **67**, 369 (2004).
- [33] X. Yan, Q. Shi, M. Hou, K. Lu, and C. K. Chan, *Phys. Rev. Lett.* **91**, 014302 (2003).
- [34] L. Reyes, I. Sánchez, and G. Gutiérrez, *Physica A* **358**, 466 (2005).
- [35] P. King, P. Lopez-Alcaraz, H. Pacheco-Martinez, C. Clement, A. Smith, and M. Swift, *Eur. Phys. J. E* **22**, 219 (2007).
- [36] H. Zhu, Z. Zhou, R. Yang, and A. Yu, *Chem. Eng. Sci.* **62**, 3378 (2007).
- [37] H. Zhu, Z. Zhou, R. Yang, and A. Yu, *Chem. Eng. Sci.* **63**, 5728 (2008).
- [38] J. Gallas, H. Herrmann, and S. Sokolowski, *Physica A* **189**, 437 (1992).
- [39] Y. Lan and A. D. Rosato, *Phys. Fluids* **7**, 1818 (1995).
- [40] J. Lee, *Physica A* **238**, 129 (1997).
- [41] T. Kawaguchi, T. Tanaka, and Y. Tsuji, *Powder Technol.* **96**, 129 (1998).
- [42] S. McNamara, E. G. Flekkøy, and K. J. Måløy, *Phys. Rev. E* **61**, 4054 (2000).
- [43] P. Biswas, P. Sanchez, M. R. Swift, and P. J. King, *Phys. Rev. E* **68**, 050301(R) (2003).
- [44] N. Burtally, P. J. King, and M. R. Swift, *Science* **295**, 1877 (2002).
- [45] E. Aharonov and D. Sparks, *Phys. Rev. E* **60**, 6890 (1999).
- [46] P. A. Cundall and O. D. Strack, *Geotechnique* **29**, 47 (1979).
- [47] This model does not include particle rotation. However it has been shown [73] that, for the cases when particles are well compacted, rotation does not affect the system significantly.
- [48] In order to choose a value of  $\gamma = \gamma_n = \gamma_s$  we performed a study of its effect on a system without air. We found that, for a fixed  $\Gamma$ , there is a critical  $\gamma$  below in which the system behaves like a granular gas and above in which there is condensed collective motion. Over the critical value, the maximum gap at the bottom becomes independent of  $\gamma$ . We selected a value of  $\gamma = 625 \text{ s}^{-1}$ . This value was low enough as to keep the restitution coefficient over 0.8, and large enough as to have no effect on the size of the gap.
- [49] D. Rapaport, *The Art of Molecular Dynamics Simulation* (Cambridge University Press, Cambridge, 1997).
- [50] A. N. Núñez, R. Darías, R. Pinto, R. Paredes V., and E. Medina, *Eur. Phys. J. E* **9**, 327 (2002).
- [51] V. Idler, Ph.D. thesis, Instituto Venezolano de Investigaciones Científicas, 2007.
- [52] Parapara is the common Venezuelan name of *Sapindus saponaria*, also known as “jaboncillo” (soap tree). The dried seed is roughly spherical, black, with diameter  $\approx 10 \text{ mm}$ .
- [53] W. Kroll, *Forsch. Geb. Ingenieurwes.* **1**, 20 (1954).
- [54] G. Gutiérrez, L. Reyes, I. Sánchez, K. Rodríguez, V. Idler, and R. Paredes, *Physica A* **356**, 83 (2005).
- [55] A. Goldshtein, M. Shapiro, L. Moldavsky, and M. Fitchman, *J. Fluid Mech.* **287**, 349 (1995).
- [56] E. Falcon, S. Fauve, and C. Laroche, *Eur. Phys. J. B* **20**, 2 (1999).
- [57] S. Luding, E. Clément, A. Blumen, J. Rajchenbach, and J. Duran, *Phys. Rev. E* **49**, 1634 (1994).
- [58] G. Scott, *Nature (London)* **188**, 908 (1960).
- [59] G. Scott, A. Charlesworth, and M. Mak, *J. Chem. Phys.* **40**, 611 (1964).
- [60] G. Scott and D. Kilgour, *J. Phys. D: Appl. Phys.* **2**, 863 (1969).
- [61] Strictly speaking we changed not only  $\rho_g$  but also the number of grains and  $d$ . However, if we keep all parameters fixed and reduce  $\rho_g$  (in the presence of air), the density of the bulk is increased [51].
- [62] K. M. Aoki and T. Akiyama, *Phys. Rev. E* **52**, 3288 (1995).
- [63] J. Bougie, Sung Joon Moon, J. B. Swift, and H. L. Swinney, *Phys. Rev. E* **66**, 051301 (2002).
- [64] K. Huang, G. Miao, P. Zhang, Y. Yun, and R. Wei, *Phys. Rev. E* **73**, 041302 (2006).
- [65] A. V. Potapov and C. S. Campbell, *Phys. Rev. Lett.* **77**, 4760 (1996).
- [66] X. Yang, C. Huan, D. Candela, R. W. Mair, and R. L. Walsworth, *Phys. Rev. Lett.* **88**, 044301 (2002).
- [67] R. D. Wildman, J. M. Huntley, J.-P. Hansen, D. J. Parker, and D. A. Allen, *Phys. Rev. E* **62**, 3826 (2000).
- [68] C. Saluena, S. E. Esipov, and T. Poeschel, *Proc. SPIE* **3045**, 2 (1997).
- [69] L. E. Silbert, D. Ertas, G. S. Grest, T. C. Halsey, and D. Levine, *Phys. Rev. E* **65**, 031304 (2002).
- [70] H. A. Makse, D. L. Johnson, and L. M. Schwartz, *Phys. Rev. Lett.* **84**, 4160 (2000).
- [71] S. F. Edwards, *Physica A* **249**, 226 (1998).
- [72] J. Sun, F. Battaglia, and S. Subramaniam, *Phys. Rev. E* **74**, 061307 (2006).
- [73] P. A. Thompson and G. S. Grest, *Phys. Rev. Lett.* **67**, 1751 (1991).